

# ON THE ORIGIN AND THE SIGNAL-SHAPING MECHANISM OF THE FAST PHOTOSIGNAL IN THE VERTEBRATE RETINA

P. HOCHSTRATE, M. LINDAU, AND H. RÜPPEL

*Max Volmer Institut für Biophysikalische und Physikalische Chemie, Technische Universität Berlin, D-1000 Berlin 12, West Germany*

**ABSTRACT** Fast photosignals (FPS) with  $R_1$  and  $R_2$  components were measured in retinas of cattle, rat, and frog within a temperature range of 0° to 60°C. Except for temperatures near 0°C the signal rise of the  $R_1$  component was determined by the duration of the exciting flash. The kinetics of the  $R_2$  component and the meta transition of rhodopsin in the cattle and rat retina were compared. For the analysis of the FPS it is presupposed that the signal is produced by light-induced charges on the outer segment envelope membrane that spread onto the whole plasma membrane of the photoreceptor cell. To a good approximation, this mechanism can be described by a model circuit with two distinct capacitors. In this model, the charging capacitance of the pigmented outer segment envelope membrane and the capacitance of the receptor's nonpigmented plasma membrane are connected via the extra- and intracellular electrolyte resistances. The active charging is explained by two independent processes, both with exponential rise ( $R_1$  and  $R_2$ ), that are due to charge displacements within the pigmented envelope membrane. The time constant  $\tau_2$  of the  $R_2$  membrane charging process shows a strong temperature dependence that of the charge redistribution,  $\tau_r$ , a weak one. In frog and cattle retinas the active charging is much slower within a large temperature range than the passive charge redistribution. From the two-capacitor model it follows for  $\tau_r \ll \tau_2$  that the rise of the  $R_2$  component is determined by  $\tau_r$ , whereas the decay is given by  $\tau_2$ . For the rat retina, however,  $\tau_2$  approaches  $\tau_r$  at physiological temperatures and becomes  $< \tau_r$  above 45°C. In this temperature range where  $\tau_2 \approx \tau_r$ , both processes affect rise and decay of the photosignal. The absolute values of  $\tau_r$  are in good accordance with the known electric parameters of the photoreceptors. At least in the cattle retina, the time constant  $\tau_2$  is identical with that of the slow component of the meta II formation. The strong temperature dependence of the meta transition time gives rise to the marked decrease of the  $R_2$  amplitude with falling temperature. As the  $R_1$  rise could not be fully time resolved the signal analysis does not yield the time constant  $\tau_1$  of the  $R_1$  generating process. It could be established, however, within the whole temperature range that the decay of the  $R_1$  component is determined by  $\tau_r$ . Using an extended model that allows for membrane leakage, we show that in normal Ringer solution the membrane time constant does not influence the signal time-course and amplitude.

## INTRODUCTION

Illuminating vertebrate photoreceptors by an intense flash of light evokes transient extracellular currents along the photoreceptors immediately after the stimulus. These currents lead to voltage changes across the extracellular resistance of the receptor layer. This fast photosignal (FPS) consists of two components with opposite polarity,  $R_1$  and  $R_2$ , whose contribution to the photosignal varies considerably with temperature (see reviews by Arden, 1969; Cone and Pak, 1971).

The current sources are assumed to be charge displacements in the plasma membrane of the outer segment, closely related to the photolysis of the visual pigment

rhodopsin (Pak, 1965; Cone, 1967; Ruppel and Hagins, 1973; Govardovskii, 1975). However, several attempts to correlate the components of the FPS with spectroscopically defined intermediates of the rhodopsin photolysis sequence did not yield unequivocal results (Cone, 1967; Ebrey, 1968; Trissl, 1979; Lindau et al., 1980). In fact, the wave form of the FPS is determined not only by the time-course of the initial charge displacements, but also by the electric properties of the photoreceptors. Thus, to separate the kinetics of the primary charge displacements from the shape of the FPS, it is necessary to study in detail how the extracellular current flow along the photoreceptors takes place.

All current models proposed to describe the electric behavior of a photoreceptor have the same main features: after light excitation, electric charge is induced on the plasma membrane of the outer segment by charge displacements within the membrane. Simultaneously, this

Dr. P. Hochstrate's present address is Visual Physiology Group, Department of Biology, University of Bochum, D-4630 Bochum 1, West Germany. Reprint requests and all inquiries should be addressed to Dr. Ruppel.

charge is redistributed by current flow via the extra- and intracellular electrolyte resistance between the membrane capacities of the rhodopsin-containing outer segment and the nonpigmented inner part of the receptor (inner segment, nucleus region, and synapse). Thus, the simplest circuit for the electrical properties of the photoreceptor is represented by two capacitors connected by two resistors.

In rat eye cups the decay time of the  $R_1$  component at 0°C coincides with that of the  $R_2$  component at 37°C. Therefore, Cone concluded that the signal decay should reflect the time constant of charge redistribution. Furthermore, at certain temperatures, the respective rise times of the  $R_1$  or the  $R_2$  component seemed to match the lumi-meta I or the meta I-meta II transitions in the rhodopsin photolysis sequence. Cone simulated photosignals between 0° and 37°C using a simple two-capacitor model, shaping the time-course of the two charge displacements according to the kinetics of the two spectroscopic transitions (Cone, 1969; Cone and Pak, 1971).

Govardovskii (1979) extended the two-capacitor model by introducing leakage conductances over the membranes. Using this model circuit he was also able to simulate the  $R_2$  wave form by charging the outer segment membrane capacity with the time constant of the meta II formation.

In two preceding papers concerning the spatial origin of the FPS, the photoreceptor was considered as a coaxial cable to describe the charge redistribution within rat rods (Hagins and Rüppel, 1971; Rüppel and Hagins, 1973). Presupposing that the outer segment cable part is charged during the meta II formation, the  $R_2$  component was computed with the result that, at least for physiological temperatures, the membrane time constant of the inner receptor part should be 10 times smaller than that of the outer segment.

A comparison of these three approaches describing the FPS wave form, shows that a fairly good signal fit with all three can be obtained although different receptor properties are used, especially with regard to the membrane time constants of outer segment and inner receptor part. Therefore, it seems the  $R_2$  component has not yet been proven to be generated by the meta transition. In any case, it has not been shown in what way the different charging and discharging processes in the photoreceptor are superimposed to yield the observed signal with its considerable temperature-dependent variation of amplitude and time-course.

#### MODEL DESCRIPTION OF THE FAST PHOTOSIGNAL

The equivalent circuit proposed by Cone (1969) for a vertebrate photoreceptor to explain the extracellular FPS is shown in Fig. 1. In this model the FPS is recorded across the extracellular resistance  $R_{ex}$ .

In the following considerations membrane conductances are omitted (i.e., leaking currents through the cell

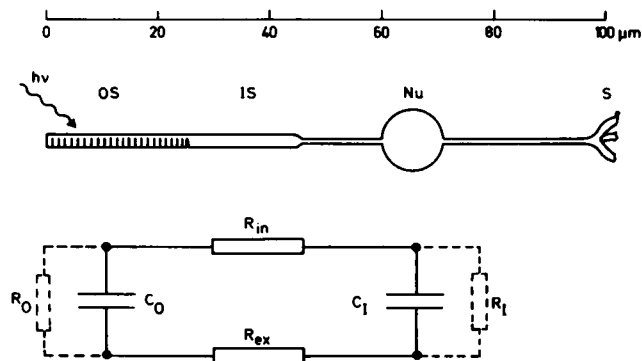


FIGURE 1 Schematic drawing of a rat rod with equivalent circuit (two-capacitor model). Above, outer segment OS; inner receptor part IS, Nu, S (inner segment, nucleus, synapse). Below,  $R_{ex}/R_{in}$  extra-/intracellular resistance;  $C_0/R_0$ ,  $C_1/R_1$  membrane capacity/resistance of outer segment, inner receptor part.

membrane are assumed not to participate in the signal-shaping mechanism). The validity of this assumption will be discussed in the Appendix. Furthermore, it is presumed that the two components of the bicomponent FPS are generated by two independent charge displacements of opposite sign, each following an exponential time-course. Consequently, the complete FPS is simply the superimposition of the single responses to each of the two charge displacements.

The membrane charge induced by a single charge displacement is given by

$$Q(t) = Q^\infty \cdot (1 - e^{-t/\tau}), \quad (1)$$

where  $Q^\infty$  is the total amount of induced charge, and  $\tau$  is the time constant of the charging process.

The intra- and extracellular resistances,  $R_{in}$  and  $R_{ex}$ , are connected in series and can be combined to  $R = R_{ex} + R_{in}$ . The redistribution current  $I = \dot{Q}_I$  is driven by the voltage drop  $U_R = U_0 - U_1$  ( $U_0$ ,  $U_1$ , membrane voltage at outer segment, inner receptor part):

$$I = \dot{Q}_I = \frac{U_R}{R} = \frac{Q_0/C_0 - Q_1/C_1}{R}, \quad (2)$$

where  $Q_0$ ,  $Q_1$  are the charges on the outer segment and inner receptor part, respectively.

With the absence of leaking currents the total charge is  $Q(t) = Q_0 + Q_1$ :

$$\begin{aligned} \dot{Q} &= \frac{C_1[Q(t) - Q_1] - C_0 Q_1}{RC_0 C_1} \\ &= \frac{C_1 Q^\infty (1 - e^{-t/\tau}) - Q_1 (C_0 + C_1)}{RC_0 C_1}. \end{aligned} \quad (3)$$

With the charge redistribution time constant

$$\tau_r = \frac{RC_0 C_1}{(C_0 + C_1)},$$

one obtains a differential equation for the charge  $Q_1(t)$  on the membrane capacity of the inner receptor part:

$$\dot{Q}_1 + \frac{1}{\tau_r} Q_1 - \frac{Q^\infty}{RC_0} (1 - e^{-t/\tau_r}) = 0. \quad (4)$$

By time differentiation, Eq. 4 yields the differential equation for the redistribution current  $I$ :

$$\dot{I} + \frac{1}{\tau_r} I - \frac{1}{\tau} \frac{Q^\infty}{RC_0} e^{-t/\tau_r} = 0, \quad (5)$$

with the solution

$$I(t) = \frac{Q^\infty}{RC_0} \cdot \frac{\tau_r}{\tau - \tau_r} (e^{-t/\tau} - e^{-t/\tau_r}). \quad (6)$$

At  $\tau$  equal  $\tau_r$ ,  $I(t)$  is given by

$$I(t) = \frac{Q^\infty}{RC_0} \cdot \frac{t}{\tau} e^{-t/\tau}. \quad (6a)$$

In Fig. 2 the charges  $Q_0$ ,  $Q_1$ , the corresponding membrane voltages  $U_0 = Q_0/C_0$ ,  $U_1 = Q_1/C_1$ , and the redistribution current are shown as a function of time for the two cases  $\tau < \tau_r$  and  $\tau > \tau_r$ .  $Q_1$  and  $Q_0$  are obtained from the integral of Eq. 6 by using Eq. 2.

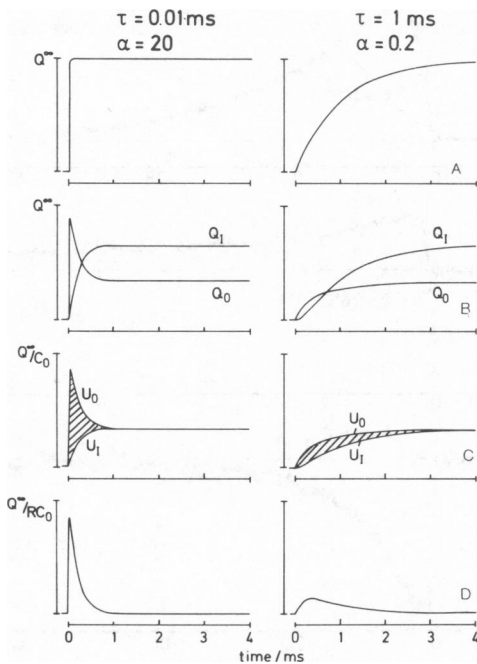


FIGURE 2 Response of the equivalent circuit given in Fig. 1 to charging of  $C_0$  with different time constants  $\tau$  at a fixed redistribution time  $\tau_r = RC_0 C_1 / (C_0 + C_1) = 0.2$  ms for  $C_0 = 2$  pF,  $C_1 = 4$  pF,  $R = R_{ex} + R_{in} = 150$  M $\Omega$  (corresponding with the known electric properties of rat rods). Left:  $\alpha = \tau_r/\tau = 20$ ; right:  $\alpha = 0.2$ . (A) Light-induced membrane charging,  $Q(t)$ ; (B) charge redistribution on outer segment and inner cell part  $Q_0(t)$ ,  $Q_1(t)$ ; (C) membrane voltage at outer segment and inner cell part  $UV_0(t)$ ,  $UV_1(t)$ ; (D) redistribution current  $I(t)$ —fast photosignal.

Obviously, the faster process determines the rise of the redistribution current and the slower one its decay. It should be noticed that with decreasing ratio  $\alpha = \tau_r/\tau$  the current maximum decreases, too. The dependence of the current maximum  $I^{\max}$  on  $\alpha$  is given by the relation

$$I^{\max} = \frac{Q^\infty}{RC_0} \cdot \alpha^{1/(1-\alpha)} \quad (7)$$

shown in Fig. 6.

Assuming two independent charge displacements with total membrane charges  $Q_1^\infty < 0$ ,  $Q_2^\infty > 0$ , and charging time constants  $\tau_1$ ,  $\tau_2$ , one obtains the total redistribution current by superposition of the single responses according to Eq. 6:

$$I(t) = \frac{\tau_r}{RC_0} \left[ Q_1^\infty \frac{e^{-t/\tau_1} - e^{-t/\tau_r}}{\tau_1 - \tau_r} + Q_2^\infty \frac{e^{-t/\tau_2} - e^{-t/\tau_r}}{\tau_2 - \tau_r} \right]. \quad (8)$$

The FPS with both components  $R_1$  and  $R_2$  is usually measured by the voltage drop  $U(t) = I(t) \cdot R_{ex}$  across the extracellular resistance  $R_{ex}$ .

The absolute value of  $\tau_r$  can be estimated using the available data of the electric properties of the photoreceptors. For rat rods the intra- and extracellular resistances have been determined by Hagins et al. (1970). With regard to the spatial dimensions of the photoreceptors (see Fig. 1) and a specific membrane capacity of  $1 \mu\text{F}/\text{cm}^2$ , the capacity of the outer segment was determined to  $C_0 = 2$  pF (15 infoldings of basal disks), and that of the inner part of the cell to  $C_1 = 4$  pF. The capacitors  $C_0$  and  $C_1$  are respectively assumed to be positioned at the middle of the outer segment (12  $\mu\text{m}$ ) and at the nucleus (60  $\mu\text{m}$ ), the latter because most of the membrane capacity of the inner cell part is concentrated in this region (see Fig. 1). The total resistance  $R$  will be given approximately by the sum of the intra- and extracellular resistances between 12 and 60  $\mu\text{m}$  that, according to Hagins et al. (1970), yields  $R \approx 150$  M $\Omega$ . In this model concept only half of the resistance of the outer segment must be considered because, on the average, the redistributed charge passes the outer segment over only half of its length. The estimated values for  $R$ ,  $C_0$ , and  $C_1$  yield  $\tau_r = 0.2$  ms. Rod receptors of cattle have shorter outer segments and smaller nuclei than those of rats (Mason, 1973; Krebs, 1981). Assuming the same resistances per length as for rats, the passive time constant  $\tau_r$  was calculated to be 0.1 ms. In the case of the cone-generated frog FPS (Goldstein, 1968; Taylor, 1969)  $\tau_r$  cannot be estimated this way because it is difficult to give a reasonable position for the model circuit elements of cones.

## METHODS AND MATERIALS

The retinas were isolated under dim red light in various Ringer solutions: cattle: 111-mM NaCl, 3.3-mM KCl, 0.36-mM  $\text{CaCl}_2$ , 0.36-mM  $\text{MgCl}_2$ , 50-mM saccharose, 7-mM phosphate buffer pH 7.2; rat: Ringer II, according to Hagins et al. (1970); frog: 119-mM NaCl, 4.7-mM KCl,

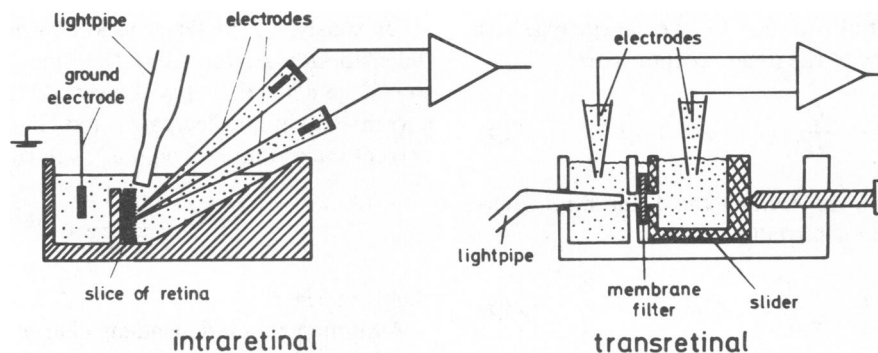


FIGURE 3 Measuring devices for recording extracellular photosignals (FPS).

2.5-mM  $\text{CaCl}_2$ , 1.2-mM  $\text{MgSO}_4$ , 1.2-mM  $\text{KH}_2\text{PO}_4$ , 24-mM  $\text{Na}_2\text{HCO}_3$ , pH 7.0.

Bovine retinas were dissected from eyes 1–3 h after enucleation in the slaughter-house. Rat and frog retinas were prepared from dark-adapted animals killed by intraperitoneal injection of Nembutal (La Société Ceva, Neuilly-sur-Seine, France) or decapitation, respectively.

For transretinal measurements, pieces of retina were attached by their vitreous sides to small squares of prewashed membrane filter (Sartorius SM 11302 or SM 11303, Sartorius Filters, Inc., Hayward, CA). These preparations were placed between the two compartments of a thermostatted chamber filled with Ringer solution (as used by Lindau et al., 1980) (see Fig. 3). White light from a xenon bulb flash tube (EG&G, Inc., Salem, MA, FX 193, rise time of flash integral  $t_f = 15 \mu\text{s}$ ) was applied through a light pipe directly onto the receptor side of the retina. The photosignals were derived by large Ag/AgCl electrodes, amplified by a difference amplifier (Tektronix AM 502, variable bandwidth, Tektronix, Inc., Beaverton, OR), and recorded by a storage oscilloscope (Tektronix 5103 N) or a signal averager (Nicolet 1072 or 1170, Nicolet Scientific Corp., Northvale, NJ). The time resolution was limited by the flash duration.

Intraretinal measurements were carried out using an experimental setup similar to that of Hagins et al. (1970). The extracellular photocurrent was observed as the potential difference between two Ringer-filled micropipette electrodes (tip diameter 3–6  $\mu\text{m}$ , resistance 1–5 M $\Omega$ ), one of which was placed at the rod tips, and the other directly beneath at a depth of 100  $\mu\text{m}$ . The electrode signals were amplified by capacitance-compensated amplifiers (AD 40K, Analog Devices, Norwood, MA). The difference signal was recorded as in the case of transretinal measurements. The maximum time resolution for microelectrode measurements was about 50  $\mu\text{s}$ . The thermostating was performed by a thermistor regulated peltier element. The temperature in the chamber was controlled by a miniature thermistor (YSI 520 with tele thermometer YSI 43 TD, Yellow Springs Instrument Co. Inc., Yellow Springs, OH). Time-course and intensity of the flash were measured by a silicon solar cell as described by Buchwald et al. (1978).

## RESULTS

The FPS was measured at different temperatures in the range from 0° to 60°C from retinas of cattle, rat, and frog. Some typical examples of these signals for the cattle retina are shown in Fig. 4. From the upper traces in this figure it can be seen that the  $R_2$  decay time is much larger than the charge redistribution time (see above). This is realized also for the frog retina <40°C and for the rat retina <35°C. In these cases, the  $R_2$  decay time could be determined by a logarithmic signal plot. The accuracy was 10–50%, depending on the decreasing  $R_2$  signal-to-noise-ratio with

falling temperature (see Fig. 4). The Arrhenius plots of the reciprocal decay time given in Fig. 5 always revealed a strong, nonlinear temperature dependence which is closely correlated with the meta transition of the rhodopsin photolysis sequence. For the cattle retina, the time constant of the slow component of the meta II formation measured in the intact retina (Schnitzkewitz, 1980) is also shown in Fig. 5. For the rat retina, however, only at 21°C have both kinetic components of the meta transition been resolved yet. In the temperature range from 30° to 40°C,

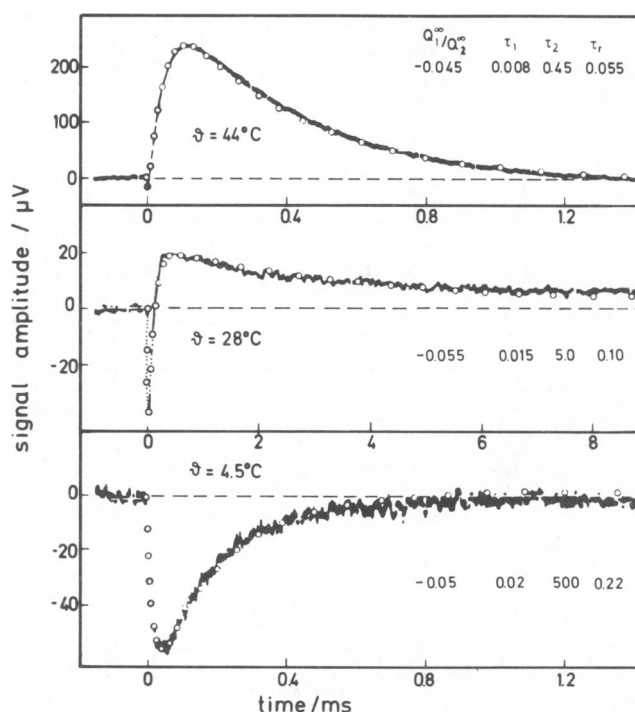


FIGURE 4 Examples for cattle transretinal photosignals at different temperatures. Bandwidth of the recording system was  $\Delta f = 30 \text{ kHz}$  for  $\vartheta = 44^\circ$  and  $4.5^\circ\text{C}$  and  $\Delta f = 10 \text{ kHz}$  for  $\vartheta = 28^\circ\text{C}$ . The fitted curve corresponding to Eq. 8a is given by open circles, the fit parameters are noted with each signal (time constants in ms). For the FPS at  $\vartheta = 4.5^\circ\text{C}$  only  $\tau_1$  and  $\tau_f$  can be determined by curve fitting;  $\tau_2$  was obtained by extrapolation of the Arrhenius plot of Fig. 5 and  $Q_1/Q_2$  was assumed to have the mean value found at higher temperatures.

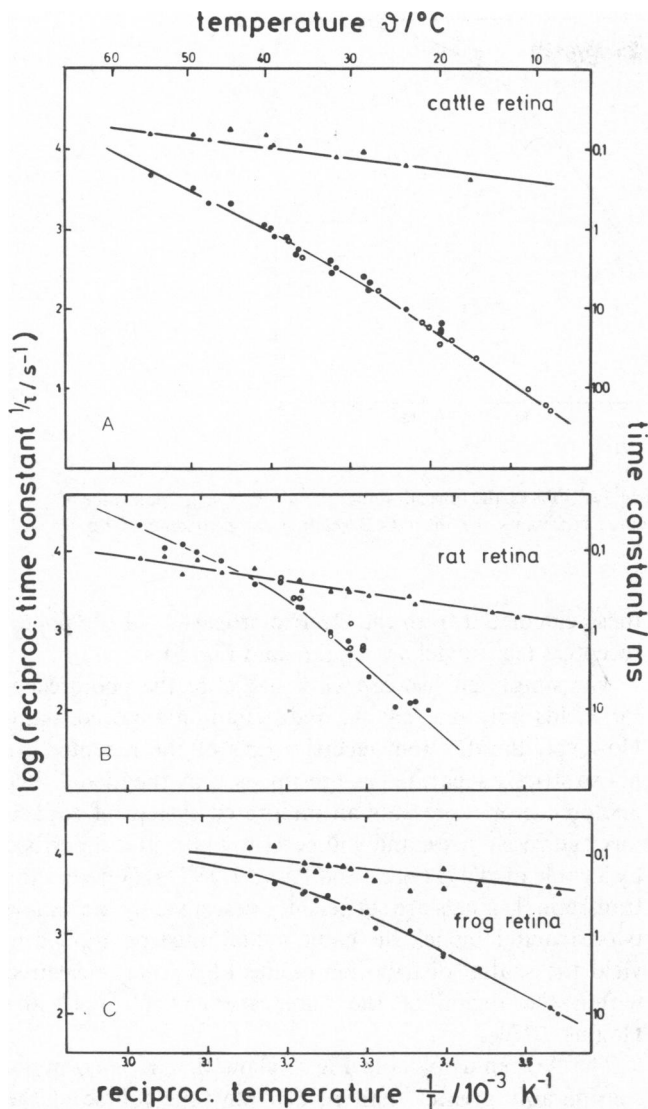


FIGURE 5 Arrhenius plots of the  $R_2$  time constants of the fast photosignal obtained from cattle, rat, and frog retinas. For A, cattle retina, the time constant of the slow component of the meta II formation is shown. For B, rat retina, the slow component is separated only at 21°C. For other temperatures only average values of the meta I decay time are measured (see text). ( $\Delta$ ) passive charge redistribution; ( $\bullet$ )  $R_2$  generating membrane charging (in B ( $\bullet$ ) signifies trans- and ( $\blacksquare$ ) inter-retinal membrane charging; ( $\circ$ ), (A) meta II-rhodopsin formation, (B) meta I-rhodopsin decay.

due to the insufficient signal-to-noise ratio, only average time constants for the meta I decay were determined.<sup>1</sup> For the frog retina no kinetic data are available on the meta reaction of the cone pigment which produces the main part of the frog FPS (Goldstein, 1968; Taylor, 1969).

The good agreement of the kinetic data in Fig. 5 strongly suggests that under these conditions the  $R_2$  gener-

ating process determines the decay rather than the rise of the  $R_2$  component. Thus  $\tau_2$  in Eq. 8 can be identified with the  $R_2$  decay time.

Normally the  $R_1$  rise was not time resolved because it was determined by the rise time  $t_f$  of the flash integral. Therefore  $\tau_1$  was substituted by the corresponding time constant  $\tau_f \approx t_f/2.2$ . If an amplifier bandwidth  $\Delta f$  lower than  $1/\tau_f$  was used,  $\tau_1$  was approximated by the band-limiting time constant (Rüppel and Witt, 1969). In the case of cattle and rat retinas at temperatures near 0°C, the  $\tau_1$  values became sufficiently large to be detectable in addition to  $\tau_f$ .

The remaining two parameters  $Q_1^\infty/Q_2^\infty$  and  $\tau_r$ , which together with  $\tau_1$  and  $\tau_2$  determine the complete signal time-course, were adjusted to fit the signal using Eq. 8 rewritten as

$$U(t) = U_2^\infty \left[ \frac{Q_1^\infty/Q_2^\infty}{\tau_1/\tau_r - 1} e^{-t/\tau_1} + \frac{1}{\tau_2/\tau_r - 1} e^{-t/\tau_2} - \left( \frac{Q_1^\infty/Q_2^\infty}{\tau_1/\tau_r - 1} + \frac{1}{\tau_2/\tau_r - 1} \right) e^{-t/\tau_r} \right]. \quad (8a)$$

$U_2^\infty = R_{ex} \cdot Q_2^\infty/RC_0$  gives the amplitude of the  $R_2$  component for  $\tau_r \rightarrow \infty$ .

At high temperatures, i.e., above 55°C for the cattle, 40°C for the frog and ~35°C for the rat retina this procedure fails because  $\tau_2$  and  $\tau_r$  both have comparable values. Therefore,  $\tau_2$  cannot be gathered simply by a logarithmic plot of the signal decay. In these cases the parameter  $\tau_2$  was also varied to fit the signal to Eq. 8a. The resulting signal time constants as given in Fig. 5 were assigned to the charge-generating or distribution process in this temperature range only by means of their different temperature dependencies.

In the Arrhenius plots of Fig. 5, the passive redistribution time constant  $\tau_r$  is easily recognized by its small, linear slope having an activation energy of ~20 kJ/mol in all three cases. In the whole temperature range  $\tau_r$  was determined with an error of about 20%. The  $Q_1^\infty/Q_2^\infty$  ratio could be evaluated only in the middle temperature range, where the  $R_1$  and  $R_2$  components have comparable amplitudes. Its error is mainly due to the deviation in the ratio  $\alpha$  of the two  $R_2$  time constants that, in this range, is <50%. The ratio  $Q_1^\infty/Q_2^\infty$  is probably temperature independent for cattle and rat and has a mean value of -0.05. For frogs  $Q_1^\infty/Q_2^\infty$  was found to change from -0.05 at 10°C to -0.2 at 40°C. For cattle and rat retinas the evaluation of the absolute signal amplitudes yields a value of  $U_2^\infty$  independent of the temperature. As  $C_0$  and  $R_{ex}/R$  should be temperature independent, it follows that  $Q_2^\infty$  is constant at least in the range from 20° to 55°C in which the  $R_2$  amplitudes could be determined with sufficient accuracy. For the frog retina, however,  $U_2^\infty$  decreases with temperature to the same extent as  $Q_1^\infty/Q_2^\infty$  increases so that only  $Q_1^\infty$  turns out to be constant.

<sup>1</sup>The rat meta I decay signals were measured by one of the authors (H. Rüppel) with W.A. Hagins during a visit to the National Institutes of Health, Bethesda, MD.

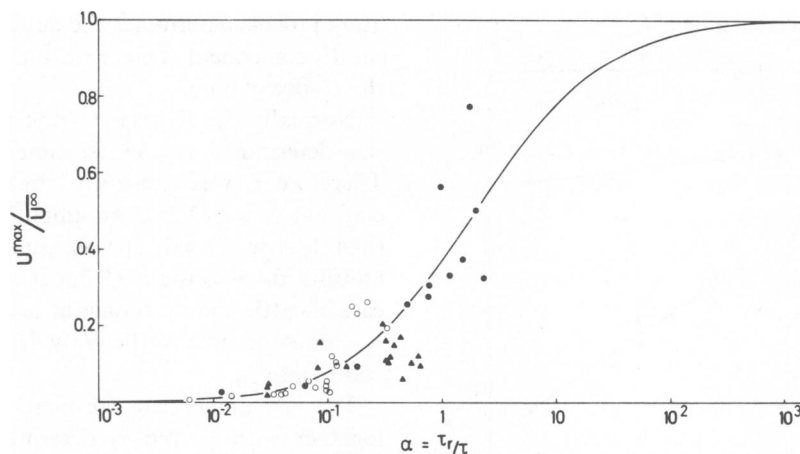


FIGURE 6 Relative  $R_2$  amplitudes  $U_2^{\max}/\bar{U}_2^\infty$  for cattle (○), rat (●), and frog (▲) FPS vs. the time constant ratio  $\alpha = \tau_r/\tau$ .  $\bar{U}_2^\infty$ , mean value of maximum  $R_2$  amplitude ( $\tau_r \rightarrow \infty$ ) for each species. The drawn out curve represents the theoretical relation corresponding to Eq. 7 ( $U_2^{\max}/\bar{U}_2^\infty = I^{\max} \cdot RC_0/Q_2^\infty = \alpha^{1/(1-\alpha)}$ ).

If  $U_2^\infty$  is independent of temperature, the amplitude of the  $R_2$  component should reflect the relation of Eq. 7. In Fig. 6 the relative  $R_2$  amplitude  $U_2^{\max}/\bar{U}_2^\infty$  for all three species is plotted vs. the ratio  $\alpha = \tau_r/\tau_2$  ( $\bar{U}_2^\infty$ , average of  $U_2^\infty$  for each species). In this diagram the  $R_2$  amplitudes were corrected to allow for the  $R_1$  influence that cannot be neglected, especially for the frog FPS, at higher temperatures. The large scatter of the  $R_2$  amplitudes is due to the different quality of the single retina preparations. Considering this inevitable amplitude scatter it is evident that the values obtained for cattle and rat are in accordance with the theoretical relation of Eq. 7. It may be noted that the frog data show a small but significant deviation from the theoretical curve, thus indicating the decrease of the  $U_2^\infty$  value with rising temperature.

## DISCUSSION

The preceding results demonstrate that the simple two-capacitor model (Fig. 1) is sufficient to describe the transretinal FPS of cattle, rat, and frog. The measured time-course of the FPS, as well as the temperature dependence of the  $R_2$  amplitude, are in good agreement with the model calculation. As shown in the Appendix, the influence of the membrane time constants on the FPS, measured in physiological Ringer solution, is not detectable within the experimental error. The time constant of the passive charge redistribution  $\tau_r = RC_0C_1/(C_0 + C_1)$  shows the expected weak temperature dependence. As the capacity of lipid bilayers is not influenced by temperature (Cole, 1968), the decrease of  $\tau_r$  with rising temperature is caused solely by that of the electrolyte resistance,  $R = R_{ex} + R_m$ . The conductance of the strong electrolytes forming the main part of the charge carriers within the retinal tissue has an activation energy of  $\sim 16$  kJ/mol, which is in accordance with the temperature dependence of  $\tau_r$ . The absolute values of  $\tau_r$  are in good agreement with

those calculated from the electric properties of the photoreceptors (see model description and Fig. 5).

The simplified two-capacitor model of the photoreceptor yields only one passive redistribution time constant. However, the different electric parts of the receptor are not so strictly separated as presupposed by the model. The photoreceptor represents an integrated system of capacitors and resistances, and will certainly be better described by a cable model (Hagins and R  ppel, 1971). Whereas the transretinal signals are sufficiently described by the simple two-capacitor model, the cable model must be applied to yield the spatial distribution of the FPS when measured within the region of the outer segment (R  ppel and Hagins, 1973).

The Arrhenius plots in Fig. 5 show that  $\tau_2$  is normally considerably greater than  $\tau_r$ , i.e., the time-course of the active membrane charging predominantly determines the  $R_2$  decay (see Fig. 2, right) (Spalink and Stieve, 1980). Only in the case of the rat retina, the Arrhenius plot of  $\tau_2$  crosses that of  $\tau_r$  at 45°C so that  $\tau_2$  becomes less than  $\tau_r$  above this temperature. Therefore, in the temperature range near 45°C in which  $\tau_2 \approx \tau_r$ , both time constants affect the rise as well as the decay of the photo signal. As shown in Fig. 2, left, at temperatures  $>55^\circ\text{C}$  the other limiting case ( $\tau_2 \ll \tau_r$ ) is being approached.

The absolute size of the FPS charge displacement can only be determined with poor accuracy. However, the calculated membrane voltages are of the same order as those measured intracellularly (Murakami and Pak, 1970; Hodgkin and O'Bryan, 1977). For transretinal signals of the rat retina the average maximum  $R_2$  amplitude  $\bar{U}_2^\infty = R_{ex}Q_2^\infty/RC_0$  was evaluated to be 1.3 mV. With  $R/R_{ex} = 0.25$  and  $C_0 = 2$  pF one obtains a total membrane charge  $Q_2^\infty = 1 \cdot 10^{-14}$  C, which corresponds to a membrane voltage change at the outer segment of about 5 mV. With 3% of the total rhodopsin ( $2 - 3 \cdot 10^7$  molecules per rod [R  ppel and Hagins, 1973]) in the plasma membrane and

a bleaching rate of 30% per flash it is estimated that one elementary charge is transported through 20% of the membrane thickness per photoactivated rhodopsin. The average  $U_2$  values for cattle (2.7 mV) and frogs (4.6 mV) are larger than for rats, which might be due to a larger resistance ratio  $R_{ex}/R$  rather than to a higher value for the induced charge per membrane area.

The comparison of the active time constant  $\tau_2$  with the spectroscopically detected reaction times of the rhodopsin intermediates can be performed most precisely for the cattle retina where rhodopsin photolysis has been carefully investigated (Stewart et al., 1977; Hoffmann et al., 1978; Schnitzkewitz, 1980). The meta I – meta II transition consists of a fast and a slow component, the amplitudes ratio of which increases with temperature. Fig. 5 shows that the slow component of the meta II formation and the  $R_2$  membrane charging have identical time constants, at least in the temperature range where both could be measured precisely. The fast component does not seem to contribute to the signal generation even at high temperatures where it constitutes the main part of the meta II signal. This does not necessarily imply that the fast meta transition is not accompanied by a charge displacement. It might be possible that the fast component occurs only in the disks but not in the plasma membrane.

As the two components of the rat meta signal could not be resolved in most cases, the reaction times given in Fig. 5 represent a mixture of the two time constants. Therefore, the meta transition appears to be slightly faster than the active membrane charging, but both temperature dependences seem to be the same. This is in agreement with the spectroscopical finding that the two components of the meta II formation have nearly the same activation energy.

The observation that, at least in the cattle retina, the slow component of the meta transition produces the  $R_2$  wave, establishes a connection between the  $R_2$  generating mechanism and the rapid calcium release which follows the slow component of the meta reaction (Kaupp et al., 1980). These findings suggest that the  $R_2$  charge displacement might change the binding constant of the calcium binding sites.

## APPENDIX

### Two-Capacitor Model Including Membrane Time Constants

The foregoing analysis of the FPS wave form suggests that leaking currents through the membranes have no influence on the signal shaping mechanism in normal Ringer solution. From intracellular FPS measurements with reptile photoreceptors (Murakami and Brown, 1970; Hodgkin and O'Bryan, 1977) the overall membrane time constant can be estimated to be at least 10 ms at room temperature. Presupposing this value for the retinas studied in this investigation, the membrane discharging process should occur ~ 20–50 times slower than the charge redistribution along the photoreceptors. This means that any amount of charge induced on the plasma membrane of the outer segment should first be redistributed over the whole receptor before it slowly disappears through the leakage conductances of the cell membrane. This consideration is generally confirmed by calculating the redistribution current on the basis of the extended two-capacitor model (Govardovskii, 1979) with membrane time constants  $\tau_0 = R_0 C_0$  for the outer segment and  $\tau_1 = R_1 C_1$  for the inner receptor part. In this case, the charge  $Q(t)$  induced on  $C_0$  is partitioned into four parts as follows:

$$Q(t) = Q_0(t) + Q_1(t) + \int_0^t i_0(t)dt + \int_0^t i_1(t)dt \quad (1A)$$

with  $i_0 = Q_0(t)/R_0 C_0$ ,  $i_1(t) = Q_1(t)/R_1 C_1$ , leakage currents through the membranes of outer segment and inner receptor part, respectively.

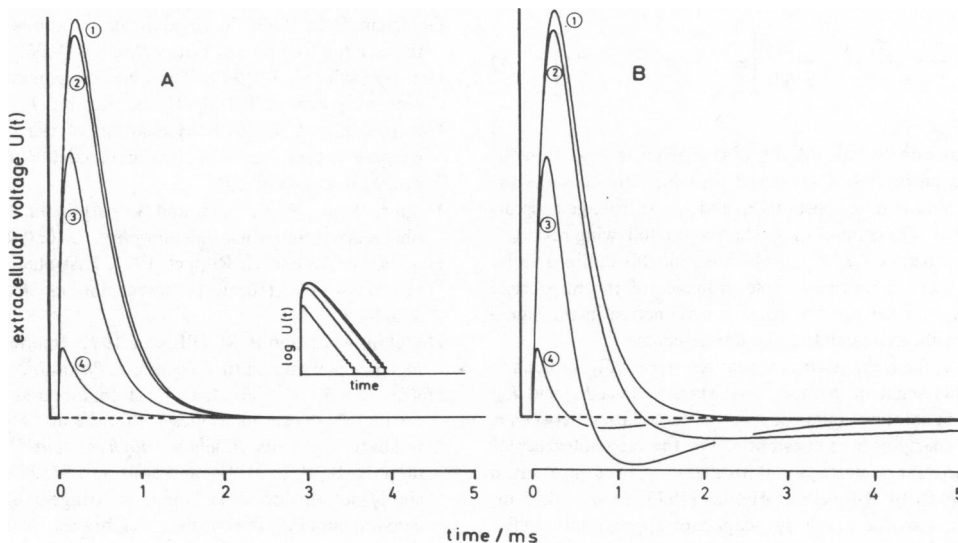


FIGURE 7 Computer simulation of FPS wave form to demonstrate the influence of the membrane time constants corresponding to Eqs. 5 and 4 of the appendix in A and B, respectively. For  $C_0$ ,  $C_1$  and  $R$  the same values are used as in Fig. 2, the time constant of membrane charging was chosen to  $\tau = 0.3$  ms. The membrane resistances  $R_0$  and  $R_1$  were varied to yield the exemplary values ① . . . ④ for  $\tau_0$  and  $\tau_1$ . (A) equal membrane time constants for outer segment and inner cell part: ①, 10 ms; ②, 2 ms; ③, 0.2 ms; ④ 0.02 ms. (B) different membrane time constants outer segment as A, inner cell part fixed to 10 ms.

Furthermore, the redistribution current  $I(t)$  via  $R$  charges not only  $C_1$  but also maintains the leakage current  $i_l(t)$ :

$$I(t) = \dot{Q}_l(t) + i_l. \quad (2A)$$

Assuming  $Q(t)$  to be exponential as in Eq. 1 of text in Model Description section, one obtains a differential equation for  $Q_l(t)$ :

$$\ddot{Q}_l + A \dot{Q}_l + B Q_l = \frac{1}{\tau} \frac{Q^\infty}{RC_0} e^{-t/\tau} \quad (3A)$$

with

$$A = \frac{1}{\tau_0} + \frac{1}{\tau_1} + \frac{1}{RC_0} + \frac{1}{RC_1},$$

$$B = \frac{1}{\tau_0\tau_1} + \frac{1}{\tau_0} RC_1 + \frac{1}{\tau_1} RC_0.$$

Together with Eq. 2A the solution of Eq. 3A yields an expression for the redistribution current  $I(t)$ :

$$I(t) = \frac{Q^\infty}{RC_0} \Omega \left[ \left( \frac{1}{\tau_1} - \frac{1}{\tau_{P_1}} \right) \theta_1 e^{-t/\tau_{P_1}} + \left( \frac{1}{\tau_1} - \frac{1}{\tau_{P_2}} \right) \theta_2 e^{-t/\tau_{P_2}} + \left( \frac{1}{\tau_1} - \frac{1}{\tau} \right) e^{-t/\tau} \right], \quad (4A)$$

where

$$\tau_{P_1} = 2(A + \sqrt{A^2 - 4B})^{-1}; \quad \tau_{P_2} = 2(A - \sqrt{A^2 - 4B})^{-1},$$

$$\theta_1 = \frac{\tau_{P_1}(\tau_{P_2} - \tau)}{\tau(\tau_{P_1} - \tau_{P_2})}, \quad \theta_2 = \frac{\tau_{P_2}(\tau_{P_1} - \tau)}{\tau(\tau_{P_2} - \tau_{P_1})},$$

$$\Omega = \frac{\tau\tau_{P_1}\tau_{P_2}}{\tau^2 - \tau\tau_{P_1} - \tau\tau_{P_2} - \tau_{P_1}\tau_{P_2}}.$$

In the symmetric case  $\tau_0 = \tau_1 \equiv \tau_M$ , Eq. 4A is reduced to a sum of two exponentials:

$$I(t) = \frac{Q^\infty}{RC_0} \cdot \frac{\tau_r\tau_M}{\tau_r\tau_r + \tau\tau_M - \tau_r\tau_M} \left[ e^{-t/\tau} - e^{-(1/\tau_r + 1/\tau_M)t} \right], \quad (5)$$

with  $\tau_r = RC_0C_1/(C_0 + C_1)$ .

A computer simulation of Eqs. 4A and 5A is given in Fig. 7 on the basis of the electric properties of a rat rod (see Fig. 2). To show the influence of the membrane time constants  $\tau_0$  and  $\tau_1$ , the leakage resistors  $R_0$  and  $R_1$  were varied. The computations showed the following results:

(a) In the symmetric case  $\tau_0 = \tau_1 \equiv \tau_M$ , which is probably realized under normal conditions, there is no measurable influence of the membrane time constant for  $\tau_M > \tau_r$ . If  $\tau_M \leq \tau_r$ , there is a reduction in the signal amplitude but no drastic change in the signal time-course.

(b) In the case  $\tau_0 > \tau_1$  the leakage current that discharges  $C_0$  is forced to flow through the inner segment membrane resistance  $R_1$  via  $R_{ex}$  and  $R_{in}$ . Its influence on the signal time-course depends on the relation between  $\tau_1$  and the membrane charging time constant  $\tau$ . For the rat photoreceptor signals with time constant values  $\tau_0 = 10$  ms and  $\tau_1 = 1$  ms (as derived from the cable model fit by R  ppel and Hagins [1973] for  $\tau = 0.35$  ms [37  C]), the difference to the simple two-capacitor approximation (Eq. 6) is not significant.

(c) In the case  $\tau_0 < \tau_1$ , there is a signal undershoot that is large if the time constant of membrane charging is of the same order of magnitude as  $\tau_0$ . This may explain the L-wave found by Yoshikami and Hagins (1973) in very low calcium Ringer, by which a high membrane conductivity of the plasma membrane is maintained in the outer segment (a corresponding

explanation was proposed before by Yoshikami in a personal communication).

The authors wish to thank Dr. W. A. Hagins, Laboratory of Chemical Physics, National Institutes of Health, Bethesda, MD, for valuable advice, and his kind permission to use rat FPS and meta transition data measured in his laboratory for this publication. These data were obtained in cooperation with Dr. H. R  ppel during two short research stays in this laboratory in 1973 and 1975. The very helpful assistance of Dr. S. Yoshikami during these experiments at the National Institutes of Health is appreciated. The authors are also grateful to Dr. M. Achtman, Max Planck Institute for Molecular Genetics, Berlin, for critical reading of the manuscript.

This work was supported by a grant to Dr. P. Hochstrate within the frame of a special research project of the Technical University Berlin, F.P.S. 6/4. The authors are also indebted for financial support given by the Fund of the German Chemical Industries, Frankfurt, West Germany.

Received for publication 7 January 1981 and in revised form 2 August 1981.

## REFERENCES

- Arden, G. B. 1969. The excitation of photoreceptors. *Prog. Biophys. Mol. Biol.* 19:373-421.
- Buchwald, H. E., P. Hochstrate, and H. R  ppel. 1978. Eine gepulste Lumineszenzdiode zur Anregung photochemischer Reaktionen in biologischen Objekten. *Feinwerktechnik und Messtechnik*. 86:270-272.
- Cole, K. S. 1968. Membranes, Ions and Impulses. University of California Press, Berkeley, CA 54.
- Cone, R. A. 1967. Early receptor potential: photoreversible charge displacement in rhodopsin. *Science (Wash. D.C.)*. 155:1128-1131.
- Cone, R. A. 1969. The early receptor potential. *Proc. Int. Sch. Phys. "Enrico Fermi."* 187-200.
- Cone, R. A., and W. L. Pak. 1971. The early receptor potential. In *Handbook of Sensory Physiology*. W. L. Loewenstein, editor. Springer-Verlag, Berlin. 1:345-365.
- Ebrey, T. G. 1968. The thermal decay of the intermediates of rhodopsin *in situ*. *Vision Res.* 8:965-981.
- Goldstein, E. B. 1968. Visual pigments and the early receptor potential of the isolated frog retina. *Vision Res.* 8:953-963.
- Govardovskii, V. I. 1975. The sites of generation of early and late receptor potentials in rods. *Vision Res.* 15:973-980.
- Govardovskii, V. I. 1979. Mechanism of the generation of the early receptor potential and an electrical model of the rod of the rat retina. *Biophysics*. 23:520-526.
- Hagins, W. A., R. D. Penn, and S. Yoshikami. 1970. Dark current and photocurrent in retinal rods. *Biophys. J.* 10:380-412.
- Hagins, W. A., and H. R  ppel. 1971. Fast photoelectric effects and the properties of vertebrate photoreceptors as electric cables. *Fed. Proc.* 30:64-68.
- Hodgkin, A. L., and P. M. O'Bryan. 1977. Internal recording of the early receptor potential in turtle cones. *J. Physiol.* 267:737-766.
- Hoffmann, W., F. Siebert, K.-P. Hofmann, and W. Kreutz. 1978. Two distinct rhodopsin molecules within the disc membranes of vertebrate rod outer segments. *Biochim. Biophys. Acta*. 503:450-461.
- Kaupp, U. B., P. P. M. Schnetkamp, and W. Junge. 1980. Metarhodopsin I/metarhodopsin II transition triggers light-induced change in calcium binding at rod disk membranes. *Nature (Lond.)*. 286:638-640.
- Krebs, W. 1982. Die Retina des Rindes. Beitrag zur Kenntnis ihrer Feinstruktur und Untersuchungen an isolierten St  bchena  ussensegmenten. Verlag Paul Parey, Berlin.
- Lindau, M., P. Hochstrate, and H. R  ppel. 1980. Two component fast photo-signals derived from rod outer segment membranes attached to



- porous cellulose filters. *FEBS (Fed. Eur. Biochem. Soc.) Lett.* 112:17–20.
- Mason, W. T. 1973. Ultrastructure of the photoreceptors of the bovine retina. In *Biochemistry and Physiology of Visual Pigments*. H. Langer, editor. Springer-Verlag, Berlin. 295–298.
- Murakami, M., and W. L. Pak. 1970. Intracellularly recorded early receptor potential of the vertebrate photoreceptors. *Vision Res.* 10:965–975.
- Pak, W. L. 1965. Some properties of the early electrical response in the vertebrate retina. *Cold Spring Harbor Symp. Quant. Biol.* 30:493–499.
- Rüppel, H., and H.-T. Witt. 1969. Measurement of fast reactions by single and repetitive excitation with pulses of electromagnetic radiation. *Methods Enzymol* 16:316–379.
- Rüppel, H., and W. A. Hagins. 1973. Spatial origin of the fast photovoltage in retinal rods. In *Biochemistry and Physiology of Visual Pigments*. H. Langer, editor. Springer-Verlag, Berlin. 257–261.
- Schnitzkewitz, G. 1980. Reaktionskinetische Untersuchungen zum Meta-Übergang der Rhodopsin-Photolyse und seine Deutung durch ein Membran-Modell. Doctoral dissertation, Technische Universität, Berlin.
- Spalink, J.-D., and H. Stieve. 1980. Direct correlation between the  $R_2$  component of the early receptor potential and the formation of metarhodopsin II in the excised bovine retina. *Biophys. Struct. Mech.* 6:171–174.
- Stewart, J. G., B. N. Baker, and T. P. Williams. 1977. Evidence for conformeric states of rhodopsin. *Biophys. Struct. Mech.* 3:19–29.
- Taylor, J. W. 1969. Cone and possible rod components of the fast photovoltage in the frog eye: a new method of measuring cone regeneration rates in vivo. *Vision Res.* 9:443–452.
- Trissl, H.-W. 1979. Light-induced conformational changes in cattle rhodopsin as probed by measurements of the interface potential. *Photochem. Photobiol.* 29:579–588.
- Yoshikami, S., and W. A. Hagins. 1973. Control of the dark current in vertebrate rods and cones. In *Biochemistry and Physiology of Visual Pigments*. H. Langer, editor. Springer-Verlag, Berlin. 245–255.